Title

Phosphoinositide Specificity of and Mechanism of Lipid Domain Formation by Annexin A2-p11 Heterotetramer*

Journal

Journal of Biological Chemistry, 280(52)

ISSN

0021-9258

Authors

Gokhale, Nikhil A

Abraham, Alexandra

Digman, Michelle A

et al.

Publication Date

2005-12-01

DOI

10.1074/jbc.m508129200

THE JOURNAL OF BIOLOGICAL CHEMISTRY VOL. 280, NO. 52, pp. 42831–42840, December 30, 2005

Phosphoinositide Specificity of and Mechanism of Lipid Domain Formation by Annexin A2-p11 Heterotetramer*

Received for publication, July 25, 2005, and in revised form, September 29, 2005 Published, JBC Papers in Press, October 17, 2005, DOI 10.1074/jbc.M508129200

Nikhil A. Gokhale[‡], Alexandra Abraham[‡], Michelle A. Digman[§], Enrico Gratton[§], and Wonhwa Cho[‡1]

From the [‡]Department of Chemistry, University of Illinois, Chicago, Illinois 60607-7061 and the [§]Department of Physics, University of Illinois, Urbana, Illinois 61801-3080

Annexin A2 is a phospholipid-binding protein that forms a heterotetramer (annexin II-p11 heterotetramer; A2t) with p11 (S100A10). It has been reported that annexin A2 is involved in binding to phosphatidylinositol 4,5-bisphosphate (PtdIns(4,5)P_2) and in inducing membrane microdomain formation. To understand the mechanisms underlying these findings, we determined the membrane binding properties of annexin A2 wild type and mutants both as monomer and as A2t. Our results from surface plasmon resonance analysis showed that A2t and annexin A2 has modest selectivity for PtdIns(4,5)P_2 over other phosphoinositides, which is conferred by conserved basic residues, including Lys[279] and Lys[281], on the convex surface of annexin A2. Fluorescence microscopy measurements using giant unilamellar vesicles showed that A2t of wild type, but not (K279A)$_2$-(p11)$_2$ or (K281A)$_2$-(p11)$_2$, specifically induced the formation of 1-μm-sized PtdIns(4,5)P_2 clusters, which were stabilized by cholesterol. Collectively, these studies elucidate the structural determinant of the PtdIns(4,5)P_2 selectivity of A2t and suggest that A2t may be involved in the regulation of PtdIns(4,5)P_2 clustering in the cell.

Annexins are a family of peripheral proteins that bind anionic phospholipids in a Ca^{2+}-dependent manner (1–5). Structures and *in vitro* functions of annexins have been well characterized. Annexins have a variable N-terminal region and a conserved C-terminal core that is composed of four (eight in case of annexin A6) α-helical annexin folds (2). The C-terminal core is the Ca^{2+}-dependent membrane-binding module that contains multiple Ca^{2+}-binding sites on its convex membrane-binding surface (2). The N-terminal region of annexins is attached to the concave side of the C-terminal core and thought to be involved in interactions with other proteins and post-translational modifications (3–5). In addition to their membrane-binding activities, annexins have been reported to have other *in vitro* activities, including membrane aggregation and lateral aggregation on the membrane surface (6). Despite the wealth of structural and functional information on annexins, their physiological functions are only beginning to emerge with recent genetic and cell studies (3–5).

Annexin A2 is an abundant cellular protein that has been implicated in numerous physiological processes (3–5, 7). Annexin A2 interacts with an EF-hand protein p11 (also known as S100A11) with high affinity via its N-terminal region, forming a symmetric heterotetramer, (annexin A2)$_2$-(p11)$_2$ (A2t)[2] (8, 9). Annexin A2 has been reported to exist either as a monomer or A2t in mammalian cells (3, 10–12). Annexin A2 and A2t have been shown to have high vesicle aggregating activity (13) and form a monolayer of protein clusters when bound to the lipid bilayer with anionic phospholipids accumulating underneath the protein clusters (14). Mounting evidence indicates that annexin A2 and A2t are involved in organizing cholesterol-rich lipid rafts (15, 16) and linking them to cytoskeletal proteins (17–20). It has been also reported that annexin A2 (21, 22) and A2t (22) bind to phosphatidylinositol 4,5-bisphosphate (PtdIns(4,5)P_2) with high specificity and affinity and that this activity is linked to the organization of actin at membrane sites that are enriched in PtdIns(4,5)P_2. Together with previous reports showing that annexin A2 binds cholesterol-containing membranes (23, 24) and PtdIns(4,5)P_2 is localized in cholesterol-rich lipid rafts in the plasma membrane (25–28), these results suggest that annexin A2 plays a role in regulating the formation of PtdIns(4,5)P_2-rich lipid rafts or lipid raft-like structures. However, it is not known whether the annexin A2 dynamically controls the organization of these structures or it passively binds to the PtdIns(4,5)P_2-rich regions. Furthermore, the affinity and specificity of annexin A2 and A2t for PtdIns(4,5)P_2 have not been quantitatively determined, which makes it difficult to assess their capability to compete with other PtdIns(4,5)P_2-binding proteins under physiological conditions.

In this study, we systematically and quantitatively determined the phosphoinositide binding specificity and affinity of annexin A2 and A2t by surface plasmon resonance (SPR) analysis and identified the structural determinant of its phosphoinositide specificity. We also investigated the formation of PtdIns(4,5)P_2-rich membrane domains on giant unilamellar vesicles (GUV) induced by A2t and mutants under various conditions. Our study provides new insight into the mechanism by which A2t mediates the organization of PtdIns(4,5)P_2-rich membrane domains.

EXPERIMENTAL PROCEDURES

Materials—1-Palmitoyl-2-oleoyl-*sn*-glycero-3-phosphocholine (POPC), 1-palmitoyl-2-oleoyl-*sn*-glycero-3-phosphoethanolamine (POPE), 1-palmitoyl-2-oleoyl-*sn*-glycero-3-phosphoserine (POPS), 1-palmitoyl-2-oleoyl-*sn*-glycero-3-phosphoinositol (POPI), and cholesterol were all purchased from Avanti Polar Lipids, Inc. (Alabaster,

* This work was supported by National Institutes of Health Grants GM52598 and GM68849 (to W. C.) and P41-RRO3155 (to E. G.). The costs of publication of this article were defrayed in part by the payment of page charges. This article must therefore be hereby marked "*advertisement*" in accordance with 18 U.S.C. Section 1734 solely to indicate this fact.

[1] To whom correspondence should be addressed: Dept. of Chemistry (M/C 111), University of Illinois, 845 W. Taylor St., Chicago, IL 60607-7061. Tel.: 312-996-4883; Fax: 312-996-2183; E-mail: wcho@uic.edu.

[2] The abbreviations used are: A2t, annexin II-p11 heterotetramer; CHAPS, 3-[(3-cholamidopropyl)dimethylammonio]-1-propanesulfonic acid; GUV, giant unilamellar vesicle(s); LUV, large unilamellar vesicle(s); PH, pleckstrin homology; PLC, phospholipase C; POPC, 1-palmitoyl-2-oleoyl-*sn*-glycero-3-phosphocholine; POPE, 1-palmitoyl-2-oleoyl-*sn*-glycero-3-phosphoethanolamine; POPI, 1-palmitoyl-2-oleoyl-*sn*-glycero-3-phosphoinositol; POPS, 1-palmitoyl-2-oleoyl-*sn*-glycero-3-phosphoserine; PtdIns(3)P, phosphatidylinositol 3-phosphate; PtdIns(4)P, phosphatidylinositol 4-phosphate; PtdIns(5)P, phosphatidylinositol 5-phosphate; PtdIns(3,4)P_2, phosphatidylinositol 3,4-bisphosphate; PtdIns(3,5)P_2, phosphatidylinositol 3,5-bisphosphate; PtdIns(3,4,5)P_3, phosphatidylinositol 3,4,5-triphosphate; PtdIns(4,5)P_2, phosphatidylinositol 4,5-bisphosphate; SPR, surface plasmon resonance; MARCKS, myristoylated alanine-rich C kinase substrate.

AL). 1,2-Dipalmitoyl derivatives of phosphatidylinositol 3-phosphate (PtdIns(3)P), phosphatidylinositol 4-phosphate (PtdIns(4)P), phosphatidylinositol 5-phosphate (PtdIns(5)P), phosphatidylinositol 3,4-bisphosphate (PtdIns(3,4)P_2), phosphatidylinositol-3,5-bisphosphate (PtdIns(3,5)P_2), PtdIns(4,5)P_2, and phosphatidylinositol-3,4,5-triphosphate (PtdIns(3,4,5)P_3) were generous gifts from Dr. Karol Bruzik. The concentrations of the phospholipids were determined by a modified Bartlett analysis (29). 6-Dodecanoyl-2-dimethylaminonaphthalene (LAURDAN), BODIPY® FL C_5,C_6-phosphatidylinositol 4,5-diphosphate (BODIPY-PtdIns(4,5)P_2), fluorescein 5-isothiocyanate ("Isomer I"), and Texas Red™ C_2-maleimide were all purchased from Invitrogen. Restriction endonucleases were purchased from New England Biolabs (Beverly, MA). CHAPS and octyl glucoside were purchased from Sigma and Fisher, respectively. The protease inhibitors, pepstatin, leupeptin, and aprotinin and the protease inhibitor mixture tablets were from Roche Applied Science. The Pioneer L1 sensor chip was purchased from Biacore AB (Piscataway, NJ).

Vector Construction and Mutagenesis—The cDNA of full-length human annexin A2, which was a generous gift from Dr. Volker Gerke, was subcloned into the vector pET-21a(+) (Novagen, Madison, WI), between the restriction sites BamHI and XhoI. A stop codon was introduced just before the restriction site XhoI in order to exclude the C-terminal hexahistidine tag from the sequence during protein expression. The cDNA of p11 (a generous gift from Dr. James Seilhamer) was also subcloned into pET-21a(+) in a similar fashion. K279A and K281A mutants of annexin A2 were generated by the overlap extension polymerase chain reaction mutagenesis. The vector pGEX-4T-1 (Novagen, Madison, WI), which has an N-terminal glutathione *S*-transferase tag and a thrombin cleavage site was used for subcloning the cDNA of the phospholipase Cδ1 (PLCδ1) pleckstrin homology (PH) domain between the restriction sites BamHI and XhoI. All of the above constructs were transformed into DH5α cells for plasmid isolation, and their DNA sequences were verified. Subsequently, these plasmids were transformed into BL21(DE3) cells for protein expression.

Protein Expression and Purification—One liter of sterile Luria broth medium containing 100 μg/ml ampicillin was inoculated with BL21(DE3) cells harboring each construct and grown at 37 °C until the optical density at 600 nm reached 0.6. Protein expression was then induced with 1 mM isopropyl-1-thio-β-D-galactopyranoside (Research Products, Mount Prospect, IL). After 8 h of incubation at 37 °C, cells were harvested by centrifugation (5,000 × *g* for 10 min at 4 °C). The resulting pellet was resuspended in 20 ml of precooled lysis buffer, containing 100 mM Tris-HCl (pH 7.5), 200 mM NaCl, 2 mM dithiothreitol, 1 mM EGTA, 0.5 mM phenylmethylsulfonyl fluoride, 5 μg/ml leupeptin, 5 μg/ml pepstatin, 5 μg/ml aprotinin, a protease inhibitor tablet, and 0.1% Triton X-100. This suspension was sonicated for 6 min (30 s of sonication followed by 30 s of incubation on ice) and then centrifuged for 1 h (40,000 × *g* at 4 °C). The supernatant was treated with 50% $(NH_4)_2SO_4$ (final concentration) for 45 min and centrifuged at 40,000 × *g* for 20 min to remove insoluble proteins. This supernatant was then applied to an 80-ml butyl-Sepharose column (Amersham Biosciences) pre-equilibrated with 50% $(NH_4)_2SO_4$ in the lysis buffer. Annexin A2 (or a mutant) was eluted with a linear gradient of $(NH_4)_2SO_4$ from 50 to 0% in the lysis buffer. The eluted samples were dialyzed against 10 mM HEPES buffer, pH 7.5, containing 50 mM NaCl, 1 mM EGTA, and 1 mM dithiothreitol and applied to a DEAE-Sepharose column (Amersham Biosciences) equilibrated with the same buffer. Elution was carried out with 200 ml of 10 mM HEPES buffer, pH 7.5, containing 1 M NaCl, 1 mM EGTA, and 1 mM dithiothreitol. The recombinant p11 was purified by the same protocol. The purified recombinant annexin A2 was dialyzed against 10 mM HEPES buffer, pH 7.5, containing 50 mM NaCl, 1 mM EGTA, 1 mM dithiothreitol, 6 mM $CaCl_2$, and a 2–5-fold molar excess of p11. These samples were then loaded onto a 5-ml Heparin HP HiTrap™ column (Amersham Biosciences) equilibrated with the same buffer without p11. The column was washed with 100 ml of the same buffer to get rid of excess p11, and the heterotetramer was eluted with 50 ml of elution buffer containing 30 mM HEPES, pH 7.5, 160 mM NaCl, 10 mM EGTA, and 1 mM dithiothreitol. The heterotetrameric nature of A2t was confirmed by the polyacrylamide gel electrophoresis performed under nondenaturing conditions (*i.e.* in the absence of SDS and dithiothreitol) using a 16% polyacrylamide gel (see Fig. 1).

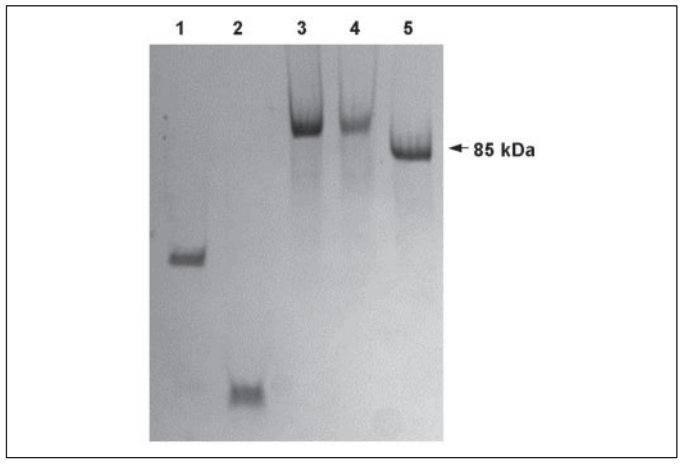

FIGURE 1. **Electropherogram of annexin A2, p11, and A2t under nondenaturing conditions.** Electrophoresis was performed using a 16% nondenaturing polyacrylamide gel and electrophoresis buffers devoid of SDS and dithiothreitol. About 20 pmol of annexin A2 (*lane 1*), p11 (*lane 2*), A2t (*lane 3*), and A2t prepared from Texas Red-labeled p11 (*lane 4*) were loaded onto the gel. Group IA cytosolic phospholipase $A_2\alpha$ (85 kDa) was used as a standard (*lane 5*). All protein samples were prepared and treated under nondenaturing conditions. Coomassie™ Blue (Amersham Biosciences) was used as a staining dye.

For the expression of the PLCδ1 PH domain, 1 liter of Luria broth containing 100 μg/ml ampicillin was inoculated with BL21(DE3) cells harboring the PH domain construct and grown at 37 °C until the optical density at 600 nm reached 0.4. Protein expression was induced by the addition of 50 mg of isopropyl-1-thio-β-D-galactopyranoside, and cells were harvested by centrifugation (5,000 × g for 10 min at 4 °C) after a 12-h incubation at 25 °C. The resulting pellet was resuspended in 10 ml of 30 mM HEPES buffer, pH 7.5, containing 160 mM NaCl, 50 μM phenylmethylsulfonyl fluoride, and 0.1% Triton X-100. This solution was sonicated for 6 min (30 s of sonication followed by 30 s of cooling on ice) and then centrifuged for 1 h (40,000 × *g* at 4 °C). After filtering the supernatant into a 50-ml Falcon tube, 500 μl of the glutathione *S*-transferase-Tag™ resin (Novagen, Madison, WI) were added. After incubating this mixture on ice for 45 min with mild shaking at 80 rpm, it was poured onto a column prerinsed with 50 ml of 30 mM HEPES buffer, pH 7.5, containing 160 mM NaCl. After washing the nonspecifically bound protein with 50 ml of 30 mM HEPES buffer, pH 7.5, containing 160 mM NaCl, 1 ml of the same buffer containing 4 units of thrombin was added in order to cleave the glutathione *S*-transferase tag, and the column was then sealed for a 6-h incubation at 25 °C. The protein was then eluted in five fractions using 500 μl of 30 mM HEPES buffer, pH 7.5, containing 160 mM NaCl. The protein purity was checked on a 16% polyacrylamide gel, and all of the protein samples were subsequently concentrated. The protein concentrations were determined by the bicinchoninic acid method (Pierce).

Chemical Labeling of Proteins—The purified p11 (2 mg/ml) was treated with a 10-fold molar excess of Texas Red™ C_2-maleimide for 2 h at room temperature in 30 mM HEPES buffer, pH 7.5, which was

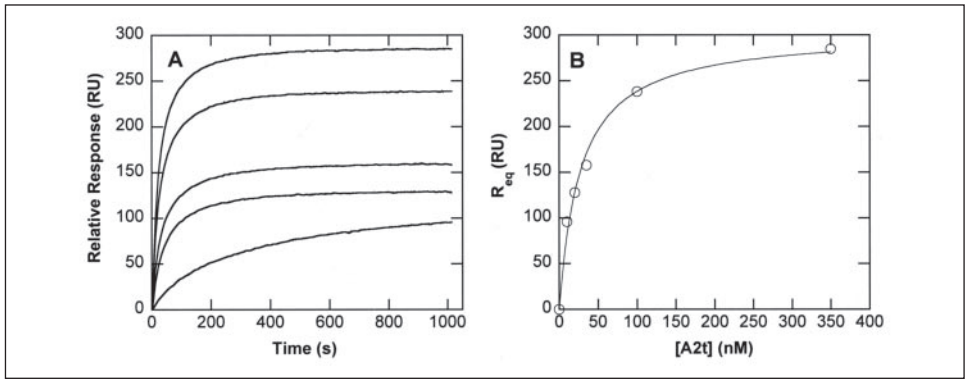

FIGURE 2. **Equilibrium SPR measurements for binding of A2t to the POPC/POPE/POPS/POPI/cholesterol/PtdIns(4,5)P$_2$ (12:35:22:6:22:3) vesicles.** *A*, SPR sensorgrams were obtained by monitoring resonance unit (*RU*) changes after injecting A2t of varying concentrations (10, 20, 35, 100, and 350 nM from *bottom* to *top*) at 5 μl/min. The R_{eq} value was graphically determined for each A2t concentration. *B*, a binding isotherm was then generated from the R_{eq} *versus* [A2t] plot. A *solid line* represents a theoretical curve constructed from R_{max} (303.46 $\pm$ 10.96) and K_d (27.35 $\pm$ 3.23 nM) values determined by nonlinear least squares analysis of the isotherm using the equation, $R_{eq} = R_{max}/(1 + K_d/C)$. 10 mM HEPES buffer, pH 7.5, with 0.16 M NaCl and 5 μM Ca^{2+} was used for this measurement.

purged with a stream of nitrogen gas before use to remove oxygen. The labeling reaction was subsequently quenched by adding an excess amount of 2-mercaptoethanol, and the labeled protein was separated from the reagents using a Sephadex G25 column (Sigma) eluted with 30 mM HEPES buffer, pH 7.5, containing 50 mM NaCl. The fractions corresponding to the protein peak were pooled and dialyzed against 30 mM HEPES buffer, pH 7.5, containing 50 mM NaCl and 6 mM $CaCl_2$ for 24 h at 4 °C. The labeling efficiency of p11 was estimated using the equation, mol of dye/mol of protein = (absorbance of the labeled protein at 582 nm)/((molar absorptivity of Texas Red at 582 nm (ϵ = 112,000 M^{-1} cm^{-1}) $\times$ (protein concentration)). Under our labeling conditions, ~0.7 mol of Texas Red was incorporated per mol of p11. The labeled p11 was then incubated on ice with purified annexin A2 (wild type or mutants) for 2 h, and the labeled heterotetramer was purified using a HiTrap™ Heparin HP column as described above. The PLCδ1 PH domain was labeled with a 10-fold molar excess of fluorescein-5-isothiocyanate for 2 h at room temperature, and the labeled protein was separated using a Sephadex G25 column eluted with 30 mM HEPES buffer, pH 7.5, containing 160 mM NaCl.

SPR Measurements—All SPR equilibrium binding measurements were carried out at 23 °C as described (30, 31). The sensor chip Pioneer L1 (Biacore) was coated with vesicles according to a protocol described previously (32). Typically, after washing the sensor chip surface, 90 μl of phospholipid vesicles of different lipid composition were injected at a flow rate of 5 μl/min to give a response of 5000 resonance units. The control surface was then coated with POPC/POPE (80:20) vesicles to give the same resonance unit response as that of the active surface. All of the equilibrium binding measurements were carried out at a steady flow rate of 5 μl/min in order to give sufficient time for the *R* values of the association phase to attain saturating response units (R_{eq}). R_{eq} values were then plotted against protein concentrations (*C*), and the K_d value was determined by a nonlinear least squares analysis of the binding isotherm using the equation $R_{eq} = R_{max}/(1 + K_d/C)$, where R_{max} is the maximal R_{eq} value.

Spectrofluorometric Measurements on Large Unilamellar Vesicles (LUV)—LUV were prepared by an extrusion method using a Liposofast microextruder and a 100-nm polycarbonate filter (Avestin, Ottawa, Canada). Spectrofluorometric measurements using LAURDAN-containing LUV were carried out with a Hitachi F4500 fluorescence spectrophotometer at an excitation wavelength of 364 nm.

Microscopy Measurements on GUV—GUV were prepared by the electroformation method using a home-built device as described previously (33). Briefly, GUV were grown in deionized water at 60 °C for 30 min by spreading ~3 μl of the lipid stock with various compositions on platinum wires. During GUV growth, the platinum wires were connected to a function generator (Hewlett-Packard, Santa Clara, CA) for 30 min, and a low frequency AC field (sinusoidal wave function with a frequency of 10 Hz and an amplitude of 3 V) was applied. After 45 min, the temperature was lowered to 40 °C, and the frequency generator was switched off after the system attained this temperature. All subsequent measurements were carried out at 40 °C in 10 mM HEPES buffer, pH 7.5, with 0.16 M NaCl and different concentrations of Ca^{2+}.

All microscopy measurements were carried out using a custom-built combination laser-scanning and multiphoton microscope that was described previously (34). Briefly, a 920-nm ultrafast pulsed beam from a tunable Tsunami laser, set up for femtosecond operation (Spectra Physics, Mountain View, CA), was spatially filtered and launched into the scan head. The beam was directed toward the primary dichroic mirror (Chroma Technology, Brattleboro, VT) and then toward the XY scan mirrors (model 6350, Cambridge Technologies, Cambridge, MA). A Prairie Technologies scan lens (Middleton, WI) was used to focus the laser light, collimated by the 1× Zeiss tube lens, and directed toward a 40× water-corrected 1.2 numerical aperture Zeiss objective, mounted on a Zeiss 200 M platform (Carl Zeiss Inc.). Light excited by a 920-nm ultrafast pulse was collected on a nondescanned pathway by the Peltier-cooled 1477P style Hamamatsu photomultiplier tubes. The light was reflected and filtered using appropriate optics. Instrument control was accomplished with the help of ISS amplifiers, an ISS three-axis scanning card (Champaign, IL), and two ISS 200-KHz analog lifetime cards. All the microscopic experiments were controlled by a data acquisition program, SimFCS (Laboratory for Fluorescence Dynamics, University of Illinois, Urbana-Champaign, IL).

RESULTS

Phosphoinositide Specificity of Annexin A2 and A2t—It has been recently reported that annexin A2 and A2t have high specificity for PtdIns(4,5)P_2 (21, 22); however, this putative PtdIns(4,5)P_2 specificity has not been quantitatively measured. We therefore prepared mixed vesicles of POPC/POPE containing 3 mol % of each of seven phosphoinositides and quantitatively determined by SPR analysis the affinity of annexin A2 and A2t for these vesicles coated onto the sensor chip. Annexin A2 and p11 have been shown to form a heterotetramer with high affinity (8, 9). Fig. 1 indicates that A2t exists as a heterotetramer under our experimental conditions. Representative sensorgrams for A2t and vesicles and a binding isotherm generated from the sensorgrams are shown in Fig. 2. The SPR method not only allows sensitive and quantitative determination of K_d values (32, 35) but also circumvents the vesicle aggregation during binding measurements, because it uses vesicles immobilized on the sensor chip. This is important, because in the vesicle pelleting assay, the charge and size of vesicles can significantly affect the pelleting efficiency, which in turn complicates the interpretation of binding data (35). For the first set of measurements, a relatively high Ca^{2+} concentration (0.1 mM) was employed to ensure that the proteins show detectable affinities for all phosphoinositide-containing vesicles

TABLE ONE

Phosphoinositide specificity for A2t, annexin A2, and p11

All binding measurements were performed in 10 mM HEPES, pH 7.5, containing 0.16 M NaCl and 0.1 mM Ca^{2+}.

Lipid composition (77:20:3)	Protein	K_d	Increase in K_d[a]
		nM	*-fold*
POPC/POPE/PtdIns(4,5)P_2	A2t	32.6 ± 2.8	1.0
POPC/POPE/PtdIns(3,4)P_2	A2t	54.6 ± 2.6	1.7
POPC/POPE/PtdIns(3,5)P_2	A2t	61.4 ± 2.1	1.9
POPC/POPE/PtdIns(3,4,5)P_3	A2t	57.1 ± 1.4	1.8
POPC/POPE/PtdIns(3)P	A2t	96.0 ± 3.3	3.0
POPC/POPE/PtdIns(4)P	A2t	126.1 ± 6.6	3.9
POPC/POPE/PtdIns(5)P	A2t	106.8 ± 4.6	3.3
POPC/POPE/POPI	A2t	360.5 ± 18	11.1
POPC/POPE/POPS	A2t	418.6 ± 26	12.8
POPC/POPE/PtdIns(4,5)P_2	A2 alone	391.6 ± 7.9	12.0
POPC/POPE/PtdIns(3)P	A2 alone	713.3 ± 9.0	21.9
POPC/POPE/PtdIns(4,5)P_2	p11 alone	758.3 ± 46.4	23.3
POPC/POPE/PtdIns(3)P	p11 alone	730.5 ± 55.3	22.4
POPC/POPE/PtdIns(4,5)P_2	PLCδ1-PH	52.0 ± 9.0	1.6

[a] -Fold increase in K_d relative to the binding of A2t to POPC/POPE/PtdIns(4,5)P_2 (77:20:3) vesicles.

under the same conditions. The control surface was coated with POPC/POPE (80:20) vesicles, because neither annexin A2 nor A2t showed detectable affinity for these zwitterionic vesicles.

As summarized in TABLE ONE, A2t showed relatively high affinity (*i.e.* K_d = 33 nM) for POPC/POPE/PtdIns(4,5)P_2 (77:20:3) vesicles, which was >10-fold higher than that for POPI- or POPS-containing vesicles. Also, this affinity is comparable with those of epsin 1 ENTH domain (36) and PLCδ1 PH domain (see TABLE ONE) for the same vesicles. However, annexin A2 monomer had >10-fold lower affinity for POPC/POPE/PtdIns(4,5)P_2 (77:20:3) vesicles than A2t under the same conditions. The difference was even bigger at lower Ca^{2+} concentrations. For instance, at 50 μM Ca^{2+}, A2t had a K_d value of ~100 nM, whereas annexin A2 monomer showed no detectable affinity, suggesting that PtdIns(4,5)P_2-dependent membrane binding of annexin A2 monomer is physiologically insignificant. We therefore focused our measurements on A2t hereafter.

When compared among phosphoinositides, A2t showed only modest selectivity for PtdIns(4,5)P_2 over other phosphoinositides (*i.e.* its affinity for PtdIns(4,5)P_2-containing vesicles was less than 2-fold higher than that for vesicles containing PtdIns(3,4)P_2, PtdIns(3,5)P_2, and PtdIns(3,4,5)P_3, respectively, and less than 4-fold higher than that for vesicles containing each monophosphorylated phosphoinositide). Under the same conditions, the annexin A2 monomer also showed modest selectivity for PtdIns(4,5)P_2 over PtdIns(3)P, whereas p11 exhibited no appreciable phosphoinositide selectivity (see TABLE ONE). To preclude the possibility that this low PtdIns(4,5)P_2 selectivity is due to our experimental conditions employing vesicles containing 3 mol % phosphoinositide, we also determined the affinity of A2t for vesicles containing 1 mol % phosphoinositide. Comparison of K_d (equal to 96.8 ± 6.7 nM) for POPC/POPE/PtdIns(4,5)P_2 (79:20:1) vesicles and K_d (equal to 156.6 ± 7.0 nM) for POPC/POPE/PtdIns(3,4)P_2 (79:20:1) vesicles showed that selectivity of A2t for PtdIns(4,5)P_2 over PtdIns(3,4)P_2 remained essentially the same regardless of the concentration of phosphoinositide in the vesicles (see also TABLE ONE). Taken together, these data show that, unlike in previous reports (21, 22), neither annexin A2 monomer nor A2t has high specificity for PtdIns(4,5)P_2. However, the finding that A2t prefers PtdIns(4,5)P_2 to more anionic PtdIns(3,4,5)P_3 indicates that the observed PtdIns(4,5)P_2 selectivity of A2t does not simply derive from nonspecific electrostatic interactions. This in turn suggests that A2t has a defined, albeit not optimized, PtdIns(4,5)P_2 binding site that is located not in p11 but in annexin A2.

The Effect of Other Lipids on Membrane Affinity of A2t—It has been reported that annexin A2 is involved in the organization of lipid rafts in the plasma membrane of mammalian cells (15, 16). To see if A2t has the physical properties that are consistent with this reported activity, we further investigated the membrane binding properties of A2t. First, we measured the affinities of A2t for the vesicles whose lipid headgroup compositions recapitulate those of mammalian cell membranes (see the footnotes to TABLE TWO) to assess the differential affinities of A2t for various cell membranes. This approach has been successfully applied to determine and account for the cellular targeting specificity of various membrane targeting domains and peripheral proteins (37, 38). For these measurements, we employed 5 μM Ca^{2+} to simulate the cellular environment as much as possible. Lower Ca^{2+} concentrations could not be used, because SPR signals were too small to analyze under such conditions.

As shown in TABLE TWO, A2t showed considerable affinity for the mimetic of inner plasma membrane at 5 μM Ca^{2+} while showing no detectable affinity for the mimetics of other cellular membranes. It should be noted that A2t exhibited no detectable binding to POPC/POPE/PtdIns(4,5)P_2 (77:20:3) vesicles at 5 μM Ca^{2+}. Therefore, A2t has a preference for the lipid composition of the inner plasma membrane, suggesting that the plasma membrane is a main site for A2t actions. This preference became more pronounced when 3 mol % PtdIns(4,5)P_2 was incorporated into the plasma membrane mimetic. The K_d value for this membrane is 27 nM even at 5 μM Ca^{2+}. Among various cellular membranes, the inner plasma membrane is known to contain the highest content of anionic lipids and cholesterol (see the footnotes to TABLE TWO), both of which have been shown to enhance the membrane affinity of annexin A2 and A2t (23, 24). To further investigate the effect of cholesterol on the membrane affinity of A2t, we measured the binding of A2 to the plasma membrane mimetic without cholesterol. A2t showed no detectable affinity for this membrane even in the presence of 3 mol % PtdIns(4,5)P_2, demonstrating the importance of cholesterol in membrane binding of A2t. Interestingly, A2t did not show any binding to POPC/POPE/cholesterol (55:20:25) vesicles even at 1 mM Ca^{2+} (data not shown), indicating that A2t does not have affinity for cholesterol

TABLE TWO

Binding affinities of A2t and mutants for cell membrane mimetics

All binding measurements were performed in 10 mM HEPES, pH 7.5, containing 0.16 M NaCl and 5 μM Ca^{2+}.

Lipid composition (77:20:3)	Protein	K_d	Increase in K_d[a]
		nM	*-fold*
PM[b]	Wild type	282.7 ± 6.2	1.0
EE[c]	Wild type	ND[d]	
NM[e]	Wild type	ND	
PM/PtdIns(4,5)P_2[f]	Wild type	27.4 ± 3.2	*0.1*[g]
PM/PtdIns(4,5)P_2-cholesterol[h]	Wild type	ND	
PM	K279A	499.7 ± 10.4	1.8
PM	K281A	804.3 ± 45.9	2.8
PM/PtdIns(4,5)P_2	K279A	447.6 ± 37.0	*1.6*[g]
PM/PtdIns(4,5)P_2	K281A	580.8 ± 17.9	*2.1*[g]

[a] -Fold increase in K_d relative to the binding of wild type A2t to PM mimetic vesicles.
[b] PM, plasma membrane-mimicking POPC/POPE/POPS/POPI/cholesterol (12:35:22:9:22) vesicles (37, 66).
[c] EE, early endosomal membrane-mimicking POPC/POPE/POPS/PtdIns(3)P (62:20:15:3) vesicles (67).
[d] ND, not detectable.
[e] NM, nuclear membrane-mimicking POPC/POPE/POPS/POPI/cholesterol (61:21:4:7:7) vesicles (37, 66).
[f] PM/PtdIns(4,5)P_2, POPC/POPE/POPS/POPI/cholesterol/PtdIns(4,5)P_2 (12:35:22:6:22:3) vesicles.
[g] Note that K279A and K281A have 16- and 21-fold lower affinities, respectively, than wild type (shown in italic numbers) under the same conditions.
[h] POPC/POPE/POPS/POPI/PtdIns(4,5)P_2 (34:35:22:6:3) vesicles.

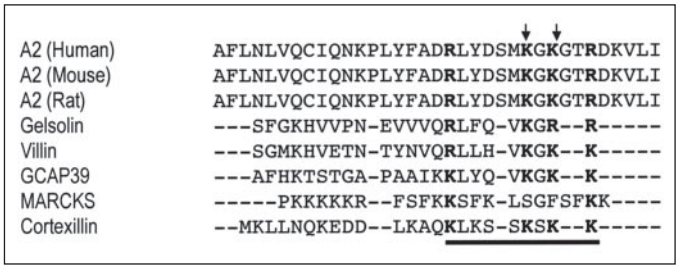

FIGURE 3. **Sequence alignment of annexin A2 with actin- and PtdIns(4,5)P_2-binding proteins.** Mammalian (human, mouse, and rat) annexin A2 sequences were aligned with gelsolin, villin, GCAP39, MARCKS, and cortexillin I. The consensus nonapeptide motif is *underlined*, and two mutated cationic residues of annexin A2 (Lys^{279} and Lys^{281}) are indicated by *arrows*.

itself. Thus, it appears that the cholesterol enhances the affinity of A2t for the plasma membrane by modulating the membrane structure.

Structural Determinant of Phosphoinositide Specificity of Annexin A2 and A2t—PtdIns(4,5)P_2-binding proteins can be subdivided into two groups (38, 39). The first group contains a well defined structural module, such as PH domain, that specifically recognizes PtdIns(4,5)P_2 in a binding pocket, whereas the second group lacks a well defined binding pocket but utilizes a cluster of surface cationic residues to bind PtdIns(4,5)P_2. Annexin 2 should belong to the second group, since it does not have an established PtdIns(4,5)P_2-binding domain. To identify the annexin A2 residues involved in PtdIns(4,5)P_2 binding, we surveyed the PtdIns(4,5)P_2-binding motifs found in several actin-binding proteins belonging to the second group, including gelsolin, villin, gCAP39, MARCKS, and cortexillin I. These proteins have a consensus nonapeptide motif, (R/K)L*XXX*(R/K)*X*(R/K)(R/K) (see Fig. 3), which is directly involved in PtdIns(4,5)P_2 binding (40, 41). A multiple sequence alignment by ClustalW (42) (Fig. 3) revealed that annexin 2 also possesses near the C terminus a putative PtdIns(4,5)P_2-binding motif. Among several conserved basic residues in this region, Lys^{279}, Lys^{281}, and Arg^{284} are located on the convex surface of the annexin core (see Fig. 4).

To see if these residues are involved in PtdIns(4,5)P_2 binding, we measured the effect of K279A and K281A mutations on the membrane affinity of A2t. R284A was not characterized, because this mutant was poorly expressed in *Escherichia coli*. When compared with A2t, $(K279A)_2$-$(p11)_2$ and $(K281A)_2$-$(p11)_2$ showed large 16- and 21-fold decreases, respectively, in the binding affinity for the plasma membrane mimetic containing 3 mol % PtdIns(4,5)P_2 at 5 μM Ca^{2+} (see TABLE TWO). When the plasma membrane mimetic was used in the absence of PtdIns(4,5)P_2, however, $(K279A)_2$-$(p11)_2$ and $(K281A)_2$-$(p11)_2$ showed less than 3-fold lower affinity than A2t. These data indicate that Lys^{279} and Lys^{281} are involved in specific PtdIns(4,5)P_2 binding rather than nonspecific binding to the anionic membrane surface.

A2t-mediated Lipid Ordering and PtdIns(4,5)P_2 Clustering—Annexin A2 has been reported to induce lipid raft formation in mammalian cells (15, 16). However, these results are based mainly on detergent extraction and antibody-mediated visualization methods, in combination with cholesterol depletion, which provide only indirect evidence and may also cause artificial lipid clustering (43). To directly measure the effects of annexin A2 and A2t on the membrane organization, we employed a well defined *in vitro* system in which interactions of A2t and annexin A2 with the vesicles of different lipid composition and sizes could be directly monitored by various fluorescence techniques. We first measured spectrofluorometrically the annexin-mediated changes in lipid ordering in the plasma membrane mimetic vesicles (LUV of 100-nm diameter) containing 3 mol % PtdIns(4,5)P_2 and 0.1 mol % LAURDAN. It has been reported (33, 44) that an increase in the membrane order causes a blue shift in the fluorescence emission of the membrane-incorporated LAURDAN. As shown in Fig. 5*A*, A2t caused a significant blue shift of the LAURDAN emission spectra, suggesting that it induces membrane ordering. In contrast, $(K279A)_2$-$(p11)_2$ (Fig. 5*B*) and $(K281A)_2$-$(p11)_2$ (Fig. 5*C*) only slightly enhanced the emission intensity without a detectable spectral shift. Neither did annexin A2 cause a significant spectral shift (data not shown). Also, we measured the effect of cholesterol on the A2t-mediated membrane ordering. As shown in Fig. 5*D*, A2t did not cause the blue shift of LAURDAN fluorescence when cholesterol was removed from the above vesicles, suggesting that the presence of cholesterol is essential for A2t-mediated membrane ordering.

We then directly monitored the A2t-mediated clustering of PtdIns(4,5)P_2 using GUV of the plasma membrane mimetic containing 1 mol % BODIPY-labeled PtdIns(4,5)P_2 and 2 mol % unlabeled PtdIns(4,5)P_2. GUV (diameter $>$ 10 μm) are an excellent model system for cell membranes that allow direct visualization of various membrane processes, including structural changes of membranes (45). For these

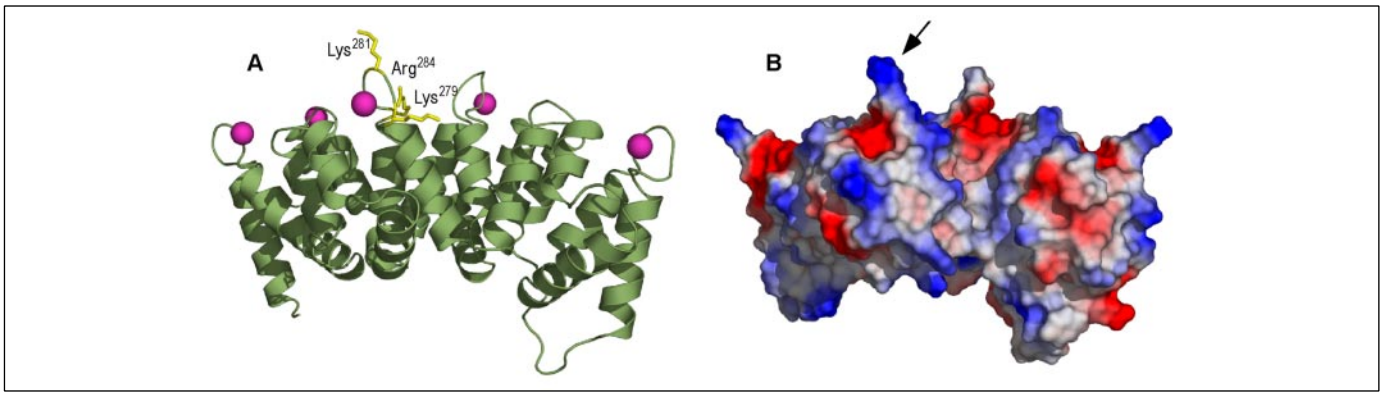

FIGURE 4. **Location of PtdIns(4,5)P_2-binding residues in annexin A2.** *A*, the structure of the C-terminal core of annexin A2 is shown in a *ribbon diagram* using atomic coordinates provided by Dr. Barbara Seaton. Three surface-exposed cationic residues in the PtdIns(4,5)P_2-binding loop, including Lys^{279} and Lys^{281}, are shown in a *yellow stick representation* and labeled. Calcium ions are shown in *magenta*. *B*, the electrostatic potential surface of the same molecule. *Red* and *blue* qualitatively indicate negative and positive electrostatic potentials, respectively. The location of the PtdIns(4,5)P_2-binding loop is indicated by the *arrow*.

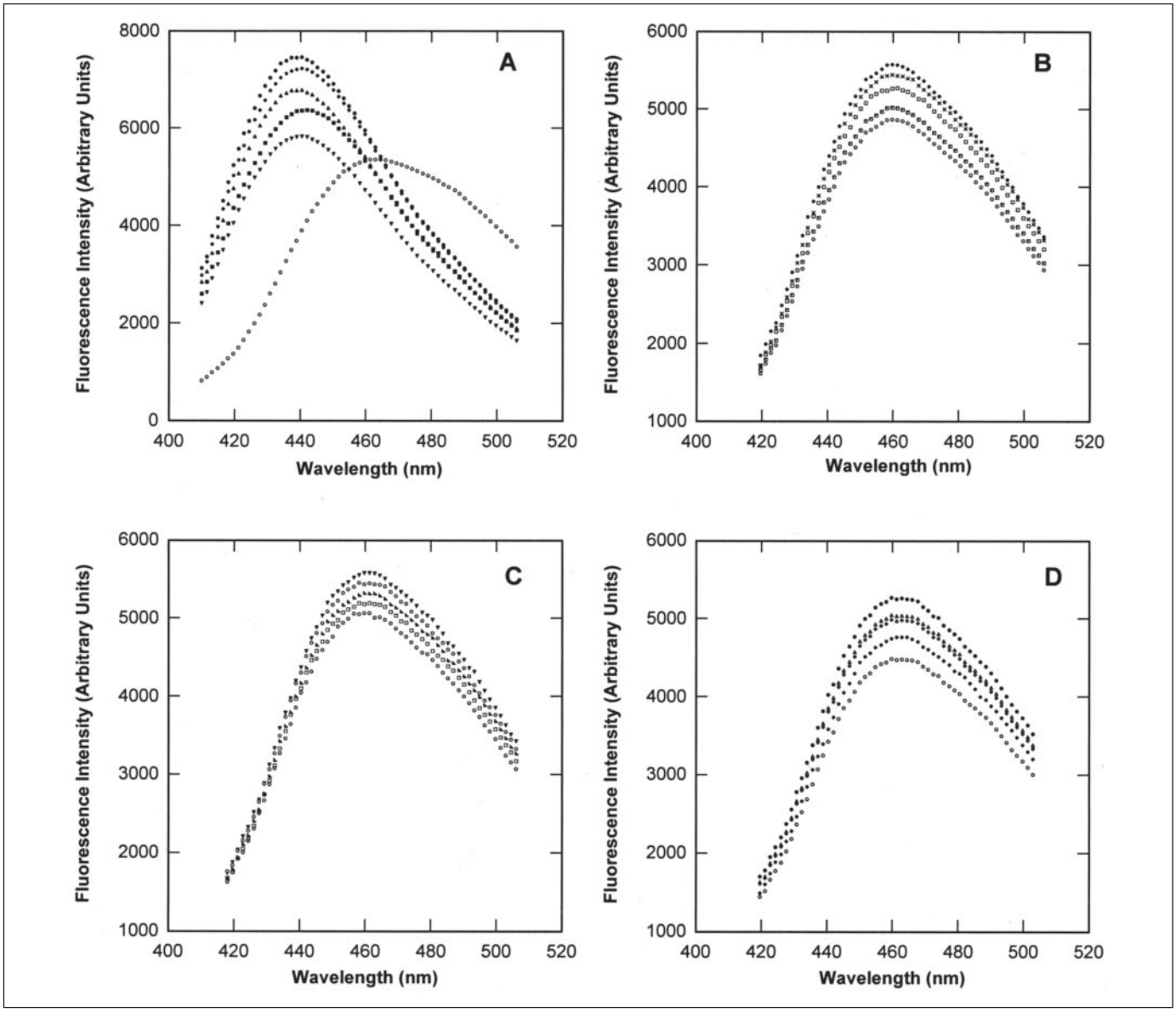

FIGURE 5. **Effects of A2t and mutants on the LAURDAN fluorescence emission spectra.** *A*, LAURDAN emission spectra in the plasma membrane-mimicking LUV containing 3 mol % PtdIns(4,5)P_2 and 0.1 mol % LAURDAN are blue-shifted after adding 40, 80, 120, 160, and 200 nM (from *bottom* to *top* in the spectra on the *left*) A2t. *B*, LAURDAN emission spectra in the same LUV after adding 0–1.0 μM (from *bottom* to *top*) $(K279A)_2$-$(p11)_2$. *C*, LAURDAN emission spectra in the same LUV after adding 0–1.0 μM (from *bottom* to *top*) $(K281A)_2$-$(p11)_2$. *D*, LAURDAN emission spectra after the addition of 0–1.0 μM (from *bottom* to *top*) of A2t to the same LUV minus cholesterol. 10 mM HEPES buffer, pH 7.5, with 0.16 M NaCl and 20 μM Ca^{2+} was used for these measurements.

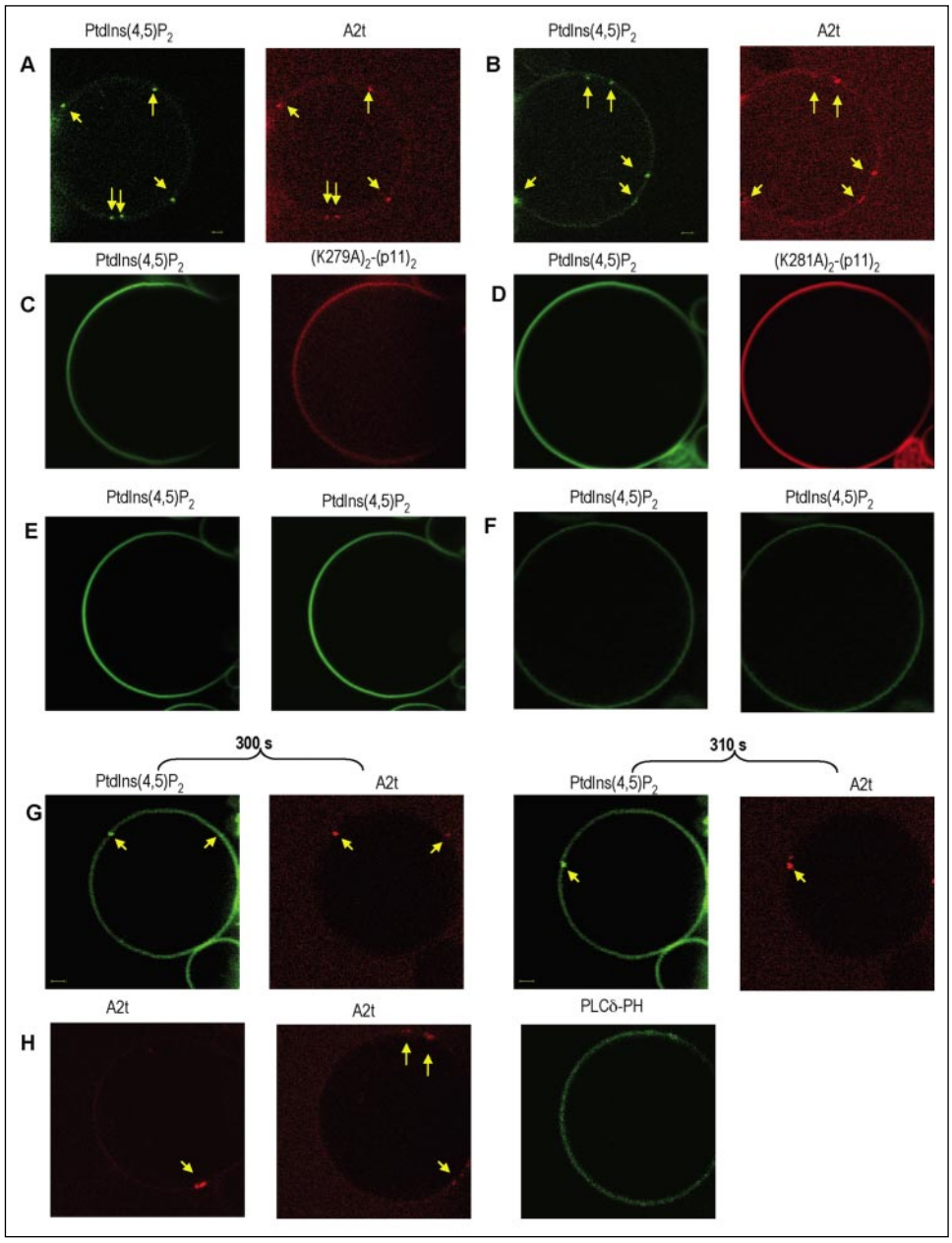

FIGURE 6. **A2t-induced PtdIns(4,5)P_2 clustering on GUV.** *A* and *B*, BODIPY-PtdIns(4,5)P_2 (*left*) and Texas Red-labeled A2t (*right*) images of two separate GUV 5 min after adding 80 nM protein. *C*, BODIPY-PtdIns(4,5)P_2 (*left*) and Texas Red-labeled (K279A)$_2$-(p11)$_2$ (*right*) images 5 min after adding 800 nM protein. *D*, BODIPY-PtdIns(4,5)P_2 (*left*) and Texas Red-labeled (K2819A)$_2$-(p11)$_2$ (*right*) images 5 min after adding 800 nM protein. *E*, BODIPY-PtdIns(4,5)P_2 images before (*left*) and 5 min after (*right*) adding 400 nM unlabeled annexin A2 monomer. *F*, BODIPY-PtdIns(4,5)P_2 images before (*left*) and 5 min after (*right*) adding 400 nM PLCδ1 PH domain. *G*, BODIPY-PtdIns(4,5)P_2 (*left*) and Texas-Red-labeled A2t (*right*) images after adding 200 nM A2t to the GUV of the plasma membrane mimetic minus cholesterol containing 1 mol % BODIPY-PtdIns(4,5)P_2 and 2 mol % unlabeled PtdIns(4,5)P_2 in 10 mM HEPES buffer, pH 7.5, with 0.16 M NaCl and 20 μM Ca^{2+}. Images are recorded at 300 and 310 s to illustrate the transient nature of the clusters. *H*, 40 nM of the labeled A2t was incubated with the GUV of the plasma membrane mimetic containing 3 mol % unlabeled PtdIns(4,5)P_2 for 20 min, and 60 nM of the labeled PH domain was added. The *left* and *middle panels* show Texas Red-labeled A2t images before and 5 min after adding the PH domain, respectively, whereas the *right panel* illustrates the labeled PH domain image 5 min after the addition. The *arrows* indicate the locations of PtdIns(4,5)P_2/A2t clusters. The GUV of the plasma membrane mimetic containing 1 mol % BODIPY-PtdIns(4,5)P_2 and 2 mol % unlabeled PtdIns(4,5)P_2 in 10 mM HEPES buffer, pH 7.5, with 0.16 M NaCl and 5 μM Ca^{2+} were used unless specified otherwise. Images were taken every 5 s.

measurements, p11 was chemically labeled with Texas Red, and this fluorescently labeled p11 was incorporated into A2t, (K279A)$_2$-(p11)$_2$, and (K281A)$_2$-(p11)$_2$, respectively. A green fluorescence protein tag on either annexin A2 or p11 could not be used here, because it interfered with heterotetramer formation and membrane binding. p11 has a single surface-exposed Cys (Cys^{82}) and another internal Cys (9). Treatment of p11 with Texas Red C_2-maleimide and partial purification yielded the labeled protein, which incorporated ~0.7 mol of Texas Red/mol of p11, implying that only Cys^{82} is labeled. Most importantly, the labeled protein formed a heterotetramer with annexin A2 (see Fig. 1), and this labeled heterotetramer was indistinguishable from the unlabeled A2t with respect to the affinity for POPC/POPE/PtdIns(4,5)P_2 (77:20:3) vesicles (K_d ~35 nM at 0.1 mM Ca^{2+}).

In the absence of proteins, the BODIPY-labeled PtdIns(4,5)P_2 showed homogeneous distribution on the GUV surfaces (Fig. 6*E*, *left*). Ca^{2+} up to 1 mM had no effect on the distribution of PtdIns(4,5)P_2 (data not shown). The addition of 80 nM A2t to the GUV in the presence of 5 μM Ca^{2+}, however, caused the formation of nearly 1-μm PtdIns(4,5)P_2 clusters (see Fig. 6, *A* and *B*, for clustering in two separate GUV). Most important, PtdIns(4,5)P_2 spots were invariably colocalized with A2t spots (Fig. 6, *A* and *B*), showing that PtdIns(4,5)P_2 clustering is directly linked to the PtdIns(4,5)P_2 binding of A2t. More than 80% of GUV used in this study showed the same trend. This notion was further supported by the finding that 300–800 nM (K279A)$_2$-(p11)$_2$ and (K281A)$_2$-(p11)$_2$ bound to GUV but did not form either PtdIns(4,5)P_2 clusters or protein aggregates under the same conditions (Fig. 6, *C* and *D*). Under the same conditions, the annexin A2 monomer (unlabeled) up to 1 μM did not cause PtdIns(4,5)P_2 clustering (Fig. 6*E*). Given that A2t has a greater tendency to laterally aggregate than annexin A2 at low Ca^{2+} concentrations (*e.g.* 5 μM), this indicates that A2t-mediated PtdIns(4,5)P_2 clustering derives not only from the capability of A2t to specifically bind PtdIns(4,5)P_2 but also from its ability to laterally aggregate on the vesicle surfaces.

To investigate the effect of cholesterol on the A2t-mediated PtdIns(4,5)P_2 clustering, we repeated the measurements using the same

GUV minus cholesterol. Since A2t has lower affinity for this membrane, Ca^{2+} concentration was raised to 20 μM (K_d ~150 nM for these vesicles at 20 μM Ca^{2+}) to facilitate the membrane binding of A2t. Under these conditions, A2t-bound GUV formed protein and PtdIns(4,5)P_2 clusters on the membrane surfaces; however, the number of clusters was significantly reduced, and the clusters were only transient, as shown by the time lapse images in Fig. 6*G*. The clusters formed in the presence of cholesterol (see Fig. 6, *A* and *B*) lasted much longer than these transient clusters. This underscores the importance of cholesterol in the formation and stabilization of the PtdIns(4,5)P_2 clusters.

Last, we measured the effect of another PtdIns(4,5)P_2-binding protein, the PH domain of PLCδ1, to see whether the PtdIns(4,5)P_2 clustering is a generic property of any PtdIns(4,5)P_2-binding proteins or specific to A2t. We incrementally added the PLCδ1 PH domain to GUV of the plasma membrane mimetic containing 1 mol % BODIPY-labeled PtdIns(4,5)P_2 and 2 mol % unlabeled PtdIns(4,5)P_2. With the PH domain concentration up to 1 μM, under which condition the vesicle surfaces should be fully covered by the PH domain (note that K_d = 52 nM for the PH domain-PtdIns(4,5)P_2 vesicle binding; see TABLE ONE), no PtdIns(4,5)P_2 clustering was detected (Fig. 6*F*). We then chemically labeled the PLCδ1 PH domain with fluorescein to simultaneously monitor vesicle binding of A2t and the PH domain. For these measurements, BODIPY-labeled PtdIns(4,5)P_2 was not included in GUV to circumvent the spectral overlap with the fluorescein-labeled PH domain. When the fluorescein-labeled PH domain was added to the mixture after the Texas Red-labeled A2t was allowed to interact with the GUV of plasma membrane mimetic containing 3 mol % unlabeled PtdIns(4,5)P_2 in the presence of 5 μM Ca^{2+}, the PH domain was able to rapidly bind to the GUV (Fig. 6*H*, *right*) without disrupting A2t clusters (Fig. 6*H*, *left* and *middle*). Notice that the locations of A2t clusters in the *left* and *middle panels* are different because they were monitored at different times, and PtdIns(4,5)P_2/A2t clusters diffused laterally on the membrane. This suggests that A2t-induced PtdIns(4,5)P_2 clusters are readily accessible to other PtdIns(4,5)P_2-binding proteins and may thus serve as sites for various PtdIns(4,5)P_2-mediated processes.

DISCUSSION

Although PtdIns(4,5)P_2 is a minor component of membrane lipids that is mainly found in the inner leaflet of plasma membrane, it plays important regulatory roles in diverse cellular processes, including actin polymerization (46, 47) and vesicle trafficking (48, 49), and also serves as the precursor for the generation of second messengers, including diacylglycerol, inositol (1,4,5)-trisphosphate (50), and PtdIns(3,4,5)P_3 (51). To account for these diverse roles of PtdIns(4,5)P_2, the presence of spatially confined PtdIns(4,5)P_2 pools in the plasma membrane has been hypothesized (48, 52, 53). Biochemical studies have indicated that PtdIns(4,5)P_2 is concentrated in membrane microdomains, such as cholesterol-rich lipid rafts (25–28). Also, direct visualization of PtdIns(4,5)P_2 by the green fluorescent protein-tagged PLCδ1 PH domain has shown the presence of PtdIns(4,5)P_2 clusters in the plasma membrane of various cells (54–57), some of which are much larger than the putative size of lipid rafts (*i.e.* <250 Å). These results indicate that PtdIns(4,5)P_2 in the plasma membrane may exist in clusters, but it is still controversial whether it is confined within the cholesterol-rich lipid rafts.

Since the rate of lateral diffusion of PtdIns(4,5)P_2 within the lipid bilayer should be much faster than the rate of its local biosynthesis (39), PtdIns(4,5)P_2 clustering would require diffusion barriers that can be provided by proteins that are capable of binding to PtdIns(4,5)P_2 and cytoskeletal proteins. Although MARCKS (39) and other proteins (58) have been implicated in reversible clustering and sequestration of PtdIns(4,5)P_2 in the plasma membrane, direct evidence for this interesting idea has not been reported. Among a large number of PtdIns(4,5)P_2-binding proteins, A2t is suited for this putative role due to its unique properties; *i.e.* A2t binds the membrane in a Ca^{2+}- and/or PtdIns(4,5)P_2-dependent manner (21, 22), laterally aggregates on the membrane surface (14), interacts with F-actin (59), and is abundant in mammalian cells. Furthermore, recent reports have indicated the potential involvement of annexin A2 and A2t in regulation of membrane microdomain formation (15, 16). The present study quantitatively shows that A2t possesses all the biophysical properties that are necessary for its putative role in organizing PtdIns(4,5)P_2 clusters in the plasma membrane and also provides direct evidence for A2t-induced PtdIns(4,5)P_2 clusters in a well defined model membrane system.

On the basis of qualitative lipid overlay assay and vesicle pelleting assay, Hayes *et al.* (21) recently reported that annexin A2 has high specificity and affinity for PtdIns(4,5)P_2. Rescher *et al.* (22) also reported that A2t as well as annexin A2 have high affinity and selectivity for PtdIns(4,5)P_2 in vesicle pelleting and lipid plate binding assays. In both studies, PtdIns(4,5)P_2 binding activity of annexin A2 and A2t was linked to the binding of these proteins to the sites of membrane-associated actin assembly in the cell. We reexamined the specificity and affinity of annexin A2 and A2t for PtdIns(4,5)P_2 by means of SPR analysis. Our SPR measurements confirm that annexin A2 and A2t bind PtdIns(4,5)P_2 and that A2t binds PtdIns(4,5)P_2-containing membranes with high affinity. The affinity of A2t for PtdIns(4,5)P_2-containing vesicles is comparable with that of the PLCδ1 PH domain and epsin ENTH domain (36). However, our measurements reveal that neither annexin A2 nor A2t has high specificity for PtdIns(4,5)P_2. The largest difference between PtdIns(4,5)P_2 and any phosphoinositide was less than 4-fold when they were incorporated in POPC/POPE/phosphoinositide (77:20:3) vesicles. This discrepancy in PtdIns(4,5)P_2 specificity between the published data and ours should arise mainly from different methods used for binding measurements (see "Results"). A typical PtdIns(4,5)P_2-specific protein, such as PLCδ1 PH domain or epsin ENTH domain (36), shows much more pronounced selectivity for PtdIns(4,5)P_2 over other phosphoinositides. Thus, cellular specificity of A2t (or annexin A2) for PtdIns(4,5)P_2 would derive from the combination of modest PtdIns(4,5)P_2 selectivity of A2t and the relative abundance of PtdIns(4,5)P_2 over other phosphoinositides. In addition, the strong preference of A2t for the inner plasma membrane over other cellular membranes should help its specific interaction with PtdIns(4,5)P_2 enriched in the plasma membrane.

There is some confusion in the literature as to whether annexin A2 monomer or A2t is involved in vesicle trafficking and membrane microdomain organization (5). As reported previously (22), the modest PtdIns(4,5)P_2 selectivity of A2t derives not from p11 but from the annexin A2 molecule. However, the affinity of annexin A2 monomer for the PtdIns(4,5)P_2-containing membrane seems to be too low to be physiologically significant. It has been long known that A2t has lower Ca^{2+} requirement for phospholipid binding and granule aggregation than annexin A2 (60). However, the difference in membrane affinity between A2t and annexin A2 has not been quantified due in part to the complication associated with a conventional vesicle pelleting assay (see "Results"). Our SPR data show that A2t has at least 10 times higher affinity for PtdIns(4,5)P_2-containing vesicles than annexin A2 at 0.1 mM Ca^{2+} and that the difference is much bigger at lower Ca^{2+} concentrations. Presumably, A2t has much higher membrane affinity than annexin A2, because two membrane binding modules of A2t function either additively or synergistically, as proposed for the membrane bind-

ing of low affinity PH domains (61). Due to its low affinity, the annexin A2 monomer would not be able to compete with other PtdIns(4,5)P_2-binding proteins for the same pools of PtdIns(4,5)P_2 unless its membrane binding is supplemented by interaction with other membrane-bound proteins. These results thus indicate that A2t is the functional form of annexin A2 in the cell as far as the PtdIns(4,5)P_2-dependent membrane binding is concerned.

This study also identifies the specific PtdIns(4,5)P_2-binding residues in the annexin A2 molecule. Annexin A2 contains the basic "nonapeptide" motif that is found in many actin- and PtdIns(4,5)P_2-binding proteins (40, 41). This motif is located in one of five Ca^{2+} binding loops. Since this loop protrudes in the middle of the convex surface (Fig. 4*A*) and has a highly positive electrostatic potential (Fig. 4*B*), it is expected to make direct contact with the anionic membrane. Among several cationic residues in this region, Lys^{279}, Lys^{281}, and Arg^{284} are surface-exposed, and at least two of them, Lys^{279} and Lys^{281}, are shown to be directly involved in PtdIns(4,5)P_2 binding. The K279A and K281A mutations reduce the affinity of A2t for the plasma membrane mimetic by less than 3-fold but decrease the affinity for the PtdIns(4,5)P_2-containing plasma membrane mimetic by about 20-fold. Thus, these residues should be directly involved in PtdIns(4,5)P_2 binding rather than interacting nonspecifically with anionic membrane surfaces. A recent crystal structure of the ANTH domain of Ap180/CALM showed that a cluster of cationic residues bind the phosphate groups of PtdIns(4,5)P_2 (62). Likewise, the surface cationic residues of annexin A2, particularly Lys^{279} and Lys^{281}, would form a surface binding site for the inositol headgroup of PtdIns(4,5)P_2. The modest phosphoinositide selectivity of annexin A2 suggests that the arrangement of these cationic residues is not fully optimized for PtdIns(4,5)P_2 binding.

The identification of PtdIns(4,5)P_2-binding residues also helped to elucidate the mechanism by which A2t induces PtdIns(4,5)P_2 clustering. A2t, but not $(K279A)_2$-$(p11)_2$ and $(K281A)_2$-$(p11)_2$, causes lipid ordering and PtdIns(4,5)P_2 clustering in LUV and GUV of the plasma membrane mimetic containing 3 mol % PtdIns(4,5)P_2. Thus, the PtdIns(4,5)P_2 binding activity of A2t appears to be essential for its effect on membrane organization. The ~1-μm size of PtdIns(4,5)P_2 clusters formed on GUV is much larger than the putative size of cholesterol-rich lipid rafts (<250 nm), indicating that the observed PtdIns(4,5)P_2 clusters do not represent the lipid raft-like structure. Since the resolution of light microscopy does not allow direct monitoring of lipid rafts, our study cannot distinguish whether A2t induces the formation of PtdIns(4,5)P_2 clusters from preexisting cholesterol- and PtdIns(4,5)P_2-rich lipid rafts or from randomly distributed lipids. In either case, the PtdIns(4,5)P_2-clustering activity of A2t would seem to derive from its ability to laterally aggregate on the membrane surface. This is because the annexin A2 monomer and the PLCδ1 PH domain, both of which bind PtdIns(4,5)P_2-containing vesicles but show little to no tendency to laterally aggregate on the membrane surface, do not show such activity.

It has been reported that cholesterol increases the affinity of annexin A2 for anionic vesicles (63) and regulates the subcellular distribution of annexin A2 (24). Our SPR measurements show, however, that annexin A2 does not bind cholesterol itself, which is consistent with a recent report on the binding of A2t to solid-supported lipid membranes (64). Thus, cholesterol should have an indirect effect on the membrane binding of A2t. It has been reported that cholesterol induces the formation of lipid microdomains (65). Therefore, cholesterol may enhance the membrane affinities of annexin A2 and A2t by mediating the formation of anionic lipid-rich microdomains and/or clusters and thereby increasing the local concentrations of anionic lipids. Our measurements show that A2t cannot effectively induce the formation of stable PtdIns(4,5)P_2 patches in the absence of cholesterol. Thus, cholesterol may play a dual role of promoting the initial membrane adsorption of A2t and facilitating the A2t-mediated formation of stable PtdIns(4,5)P_2 patches.

On the basis of our results and known properties of other PtdIns(4,5)P_2-binding proteins (38), we propose the mechanism by which A2t induces PtdIns(4,5)P_2 clustering in model membranes. A2t binds to anionic membranes via Ca^{2+}-dependent nonspecific electrostatic interactions. This initial binding is followed by lateral diffusion of A2t on the membrane surface to specifically bind PtdIns(4,5)P_2. As A2t molecules laterally aggregate on the membrane surface, protein-bound PtdIns(4,5)P_2 molecules also form patches, which is facilitated by the presence of cholesterol in the membrane. These A2t-induced PtdIns(4,5)P_2 clusters are still accessible to other PtdIns(4,5)P_2-binding proteins, as evidenced by undeterred binding of the PLCδ1 PH domain to the PtdIns(4,5)P_2 clusters. In the cell, A2t is expected to bind the plasma membrane (or early endosomes under certain conditions) containing PtdIns(4,5)P_2 and cause similar PtdIns(4,5)P_2 clustering in a Ca^{2+}-dependent manner, thereby generating spatially separated PtdIns(4,5)P_2 pools. In this case, dual interactions of A2t with both the membrane and the cytoskeleton will severely limit the mobility of PtdIns(4,5)P_2 clusters. Whether these PtdIns(4,5)P_2 clusters correspond to lipid rafts or not, they may function as the sites for cell signaling, vesicle trafficking, or actin assembly. Obviously, further studies are necessary to elucidate if and how A2t mediates PtdIns(4,5)P_2 clustering in the cell. This *in vitro* study provides important new structural and mechanistic information that will form the basis of such cell studies.

Acknowledgments—We thank Dr. Barbara Seaton for allowing use of the coordinates of annexin A2 prior to publication.

REFERENCES

1. Creutz, C. E. (1992) *Science* **258,** 924–931
2. Swairjo, M. A., and Seaton, B. A. (1994) *Annu. Rev. Biophys. Biomol. Struct.* **23,** 193–213
3. Gerke, V., and Moss, S. E. (2002) *Physiol. Rev.* **82,** 331–371
4. Rescher, U., and Gerke, V. (2004) *J. Cell Sci.* **117,** 2631–2639
5. Gerke, V., Creutz, C. E., and Moss, S. E. (2005) *Nat. Rev. Mol. Cell Biol.* **6,** 449–461
6. Gerke, V., and Moss, S. E. (1997) *Biochim. Biophys. Acta.* **1357,** 129–154
7. Waisman, D. M. (1995) *Mol. Cell Biochem.* **149,** 301–322
8. Johnsson, N., Marriott, G., and Weber, K. (1988) *EMBO J.* **7,** 2435–2442
9. Rety, S., Sopkova, J., Renouard, M., Osterloh, D., Gerke, V., Tabaries, S., Russo-Marie, F., and Lewit-Bentley, A. (1999) *Nat. Struct. Biol.* **6,** 89–95
10. Harder, T., and Gerke, V. (1994) *Biochim. Biophys. Acta.* **1223,** 375–382
11. Nilius, B., Gerke, V., Prenen, J., Szucs, G., Heinke, S., Weber, K., and Droogmans, G. (1996) *J. Biol. Chem.* **271,** 30631–30636
12. Konig, J., Prenen, J., Nilius, B., and Gerke, V. (1998) *J. Biol. Chem.* **273,** 19679–19684
13. Raynal, P., and Pollard, H. B. (1994) *Biochim. Biophys. Acta.* **1197,** 63–93
14. Menke, M., Ross, M., Gerke, V., and Steinem, C. (2004) *Chembiochem* **5,** 1003–1006
15. Oliferenko, S., Paiha, K., Harder, T., Gerke, V., Schwarzler, C., Schwarz, H., Beug, H., Gunthert, U., and Huber, L. A. (1999) *J. Cell Biol.* **146,** 843–854
16. Babiychuk, E. B., and Draeger, A. (2000) *J. Cell Biol.* **150,** 1113–1124
17. Harder, T., Kellner, R., Parton, R. G., and Gruenberg, J. (1997) *Mol. Biol. Cell* **8,** 533–545
18. Merrifield, C. J., Rescher, U., Almers, W., Proust, J., Gerke, V., Sechi, A. S., and Moss, S. E. (2001) *Curr. Biol.* **11,** 1136–1141
19. Zobiack, N., Rescher, U., Laarmann, S., Michgehl, S., Schmidt, M. A., and Gerke, V. (2002) *J. Cell Sci.* **115,** 91–98
20. Benaud, C., Gentil, B. J., Assard, N., Court, M., Garin, J., Delphin, C., and Baudier, J. (2004) *J. Cell Biol.* **164,** 133–144
21. Hayes, M. J., Merrifield, C. J., Shao, D., Ayala-Sanmartin, J., Schorey, C. D., Levine, T. P., Proust, J., Curran, J., Bailly, M., and Moss, S. E. (2004) *J. Biol. Chem.* **279,** 14157–14164
22. Rescher, U., Ruhe, D., Ludwig, C., Zobiack, N., and Gerke, V. (2004) *J. Cell Sci.* **117,** 3473–3480
23. Ayala-Sanmartin, J., Henry, J. P., and Pradel, L. A. (2001) *Biochim. Biophys. Acta.* **1510,** 18–28
24. Mayran, N., Parton, R. G., and Gruenberg, J. (2003) *EMBO J.* **22,** 3242–3253

25. Pike, L. J., and Casey, L. (1996) *J. Biol. Chem.* **271,** 26453–26456
26. Pike, L. J., and Miller, J. M. (1998) *J. Biol. Chem.* **273,** 22298–22304
27. Waugh, M. G., Lawson, D., Tan, S. K., and Hsuan, J. J. (1998) *J. Biol. Chem.* **273,** 17115–17121
28. Waugh, M. G., Minogue, S., Anderson, J. S., dos Santos, M., and Hsuan, J. J. (2001) *Biochem. Soc. Trans.* **29,** 509–511
29. Kates, M. (1986) *Techniques of Lipidology*, 2nd Ed., Elsevier, Amsterdam, The Netherlands
30. Ananthanarayanan, B., Stahelin, R. V., Digman, M. A., and Cho, W. (2003) *J. Biol. Chem.* **278,** 46886–46894
31. Stahelin, R. V., Long, F., Diraviyam, K., Bruzik, K. S., Murray, D., and Cho, W. (2002) *J. Biol. Chem.* **277,** 26379–26388
32. Stahelin, R. V., and Cho, W. (2001) *Biochemistry* **40,** 4672–4678
33. Bagatolli, L. A., and Gratton, E. (1999) *Biophys. J.* **77,** 2090–2101
34. Stahelin, R. V., Digman, M. A., Medkova, M., Ananthanarayanan, B., Rafter, J. D., Melowic, H. R., and Cho, W. (2004) *J. Biol. Chem.* **279,** 29501–29512
35. Cho, W., Bittova, L., and Stahelin, R. V. (2001) *Anal. Biochem.* **296,** 153–161
36. Stahelin, R. V., Long, F., Peter, B. J., Murray, D., De Camilli, P., McMahon, H. T., and Cho, W. (2003) *J. Biol. Chem.* **278,** 28993–28999
37. Stahelin, R. V., Rafter, J. D., Das, S., and Cho, W. (2003) *J. Biol. Chem.* **278,** 12452–12460
38. Cho, W., and Stahelin, R. V. (2005) *Annu. Rev. Biophys. Biomol. Struct.* **34,** 119–151
39. McLaughlin, S., Wang, J., Gambhir, A., and Murray, D. (2002) *Annu. Rev. Biophys. Biomol. Struct.* **31,** 151–175
40. Janmey, P. A., Lamb, J., Allen, P. G., and Matsudaira, P. T. (1992) *J. Biol. Chem.* **267,** 11818–11823
41. Stock, A., Steinmetz, M. O., Janmey, P. A., Aebi, U., Gerisch, G., Kammerer, R. A., Weber, I., and Faix, J. (1999) *EMBO J.* **18,** 5274–5284
42. Chenna, R., Sugawara, H., Koike, T., Lopez, R., Gibson, T. J., Higgins, D. G., and Thompson, J. D. (2003) *Nucleic Acids Res.* **31,** 3497–3500
43. van Rheenen, J., Achame, E. M., Janssen, H., Calafat, J., and Jalink, K. (2005) *EMBO J.* **24,** 1664–1673
44. Dietrich, C., Bagatolli, L. A., Volovyk, Z. N., Thompson, N. L., Levi, M., Jacobson, K., and Gratton, E. (2001) *Biophys. J.* **80,** 1417–1428
45. Menger, F. M., and Keiper, J. S. (1998) *Curr. Opin. Chem. Biol.* **2,** 726–732
46. Czech, M. P. (2000) *Cell* **100,** 603–606
47. Caroni, P. (2001) *EMBO J.* **20,** 4332–4336
48. Martin, T. F. (2001) *Curr. Opin. Cell Biol.* **13,** 493–499
49. Roth, M. G. (2004) *Physiol. Rev.* **84,** 699–730
50. Berridge, M. J., and Irvine, R. F. (1984) *Nature* **312,** 315–321
51. Rameh, L. E., and Cantley, L. C. (1999) *J. Biol. Chem.* **274,** 8347–8350
52. Simonsen, A., Wurmser, A. E., Emr, S. D., and Stenmark, H. (2001) *Curr. Opin. Cell Biol.* **13,** 485–492
53. Janmey, P. A., and Lindberg, U. (2004) *Nat. Rev. Mol. Cell Biol.* **5,** 658–666
54. Botelho, R. J., Teruel, M., Dierckman, R., Anderson, R., Wells, A., York, J. D., Meyer, T., and Grinstein, S. (2000) *J. Cell Biol.* **151,** 1353–1368
55. Terebiznik, M. R., Vieira, O. V., Marcus, S. L., Slade, A., Yip, C. M., Trimble, W. S., Meyer, T., Finlay, B. B., and Grinstein, S. (2002) *Nat. Cell Biol.* **4,** 766–773
56. Watt, S. A., Kular, G., Fleming, I. N., Downes, C. P., and Lucocq, J. M. (2002) *Biochem. J.* **363,** 657–666
57. Huang, S., Lifshitz, L., Patki-Kamath, V., Tuft, R., Fogarty, K., and Czech, M. P. (2004) *Mol. Cell Biol.* **24,** 9102–9123
58. Laux, T., Fukami, K., Thelen, M., Golub, T., Frey, D., and Caroni, P. (2000) *J. Cell Biol.* **149,** 1455–1472
59. Filipenko, N. R., and Waisman, D. M. (2001) *J. Biol. Chem.* **276,** 5310–5315
60. Drust, D. S., and Creutz, C. E. (1988) *Nature* **331,** 88–91
61. Klein, D. E., Lee, A., Frank, D. W., Marks, M. S., and Lemmon, M. A. (1998) *J. Biol. Chem.* **273,** 27725–27733
62. Ford, M. G., Pearse, B. M., Higgins, M. K., Vallis, Y., Owen, D. J., Gibson, A., Hopkins, C. R., Evans, P. R., and McMahon, H. T. (2001) *Science* **291,** 1051–1055
63. Ayala-Sanmartin, J. (2001) *Biochem. Biophys. Res. Commun.* **283,** 72–79
64. Ross, M., Gerke, V., and Steinem, C. (2003) *Biochemistry* **42,** 3131–3141
65. Brown, D. A., and London, E. (1998) *Annu. Rev. Cell Dev. Biol.* **14,** 111–136
66. McMurray, W. C. (1973) in *Form and Function of Phospholipids* (Ansell, G. B., Hawthorne, J. N., and Dawson, R. M. C., eds) pp. 205–251, Elsevier, Amsterdam, The Netherlands
67. Kobayashi, T., Stang, E., Fang, K. S., de Moerloose, P., Parton, R. G., and Gruenberg, J. (1998) *Nature* **392,** 193–197

Phosphoinositide Specificity of and Mechanism of Lipid Domain Formation by Annexin A2-p11 Heterotetramer

Nikhil A. Gokhale, Alexandra Abraham, Michelle A. Digman, Enrico Gratton and Wonhwa Cho

J. Biol. Chem. 2005, 280:42831-42840.
doi: 10.1074/jbc.M508129200 originally published online October 17, 2005
